Offshore and onshore wind turbine wake meandering studied in an ABL wind tunnel

Barlas, Emre; Buckingham, Sophia ; Glabeke, Gertjan ; van Beeck, Jeroen

Published in:
Proceedings. International Workshop on Physical Modeling of Flow and Dispersion Phenomena (PHYSMOD)

Publication date:
2015

Document Version
Peer reviewed version

Offshore and onshore wind turbine wake meandering studied in an ABL wind tunnel

Emre Barlas[a], *Sophia Buckingham*[b], *Gertjan Glabeke*[b], *Jeroen van Beeck*[b]

[a]DTU, Denmark
[b]von Karman Institute for Fluid Dynamics, Belgium, vanbeeck@vki.ac.be

ABSTRACT
Scaled wind turbine models have been installed in the VKI L1-B atmospheric boundary layer wind tunnel at offshore and onshore conditions. Time-resolved measurements were carried out with three component hot wire anemometry and stereo-PIV in the middle vertical plane of the wake up to eleven turbine diameter downstream. The results show an earlier wake recovery for the onshore case. The effect of inflow conditions and the wind turbine's working conditions on wake meandering was investigated. Wake meandering was detected by hot wire anemometry through a low frequency peak in the turbulent power spectrum, present in the entire wake mainly for offshore inflow condition. It was found that the Strouhal number, based on the rotor diameter and the wind velocity at hub height, was in the order of 0.25.
Below the meandering frequency, turbulence power spectrum decreased, whereas above it increased. Wake meandering did not persist strongly further downstream in the wind farm layout studied.

1 INTRODUCTION

The number of wind farms are increasing day by day resulting in turbines that are situated in a more clustered manner. This grouping gives rise to two main disadvantages in terms of cost of energy. First, the wind-speed caused by the upstream turbines leaves less wind power to produce for the downstream ones. Secondly, increased turbulence decreases the lifetime of downstream turbines due to increased fatigue. A deep enough understanding has not been fully reached (Crespo et al. 1999; Sanderse et al. 2011). CFD computations by Church-field et al. (2012) conclude that the loading on the turbine caused by large coherent turbulent structures generated at certain conditions of the atmospheric boundary-layer are at least as important as small-scale wake-induced loading. Medici and Alfredsson (2006) link meandering behaviour to the intrinsic instabilities as in bluff body vortex shedding even though it has been contradicted by Larsen et al. (2008) and Devinant et al. (2011). The aim of this work is to provide additional data to the existing experimental wake database with tailored-designed rotating turbine models and state-of-the-art experimental techniques. The meandering phenomenon was investigated through the spectral content analysis.

2 WIND TURBINE FOR ABL WIND TUNNEL

The wind turbine model is depicted in Figure 1. It has been designed by Blade Element Momentum theory with the objective to maximize the power coefficient $Cp_{electric}$. Due to the much lower Reynolds numbers involved (~10^5), the relative blade chords are much larger whereas the blade thickness is much smaller than a real-size wind turbine. The maximum $Cp_{electric}$ is reached for a tip-speed ratio of ~5, which has been obtained by varying the electric

resistance (Figure 2). This tip-speed ratio thus the thrust was kept constant during the wind turbine study. More details on the model wind turbine are given in Barlas et al. (2015).

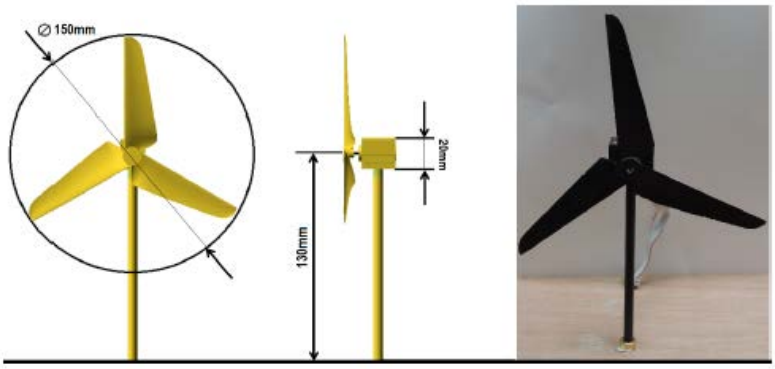

Figure 1: wind turbine model and mast dimensions.

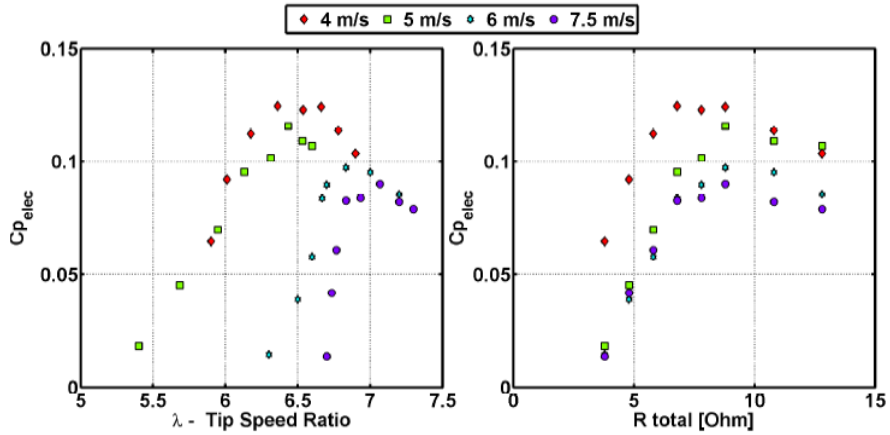

Figure 2: $Cp_{electric}$ as a function of Tip Speed Ratio (left) and Resistance (right) for 4 different velocities at hub height.

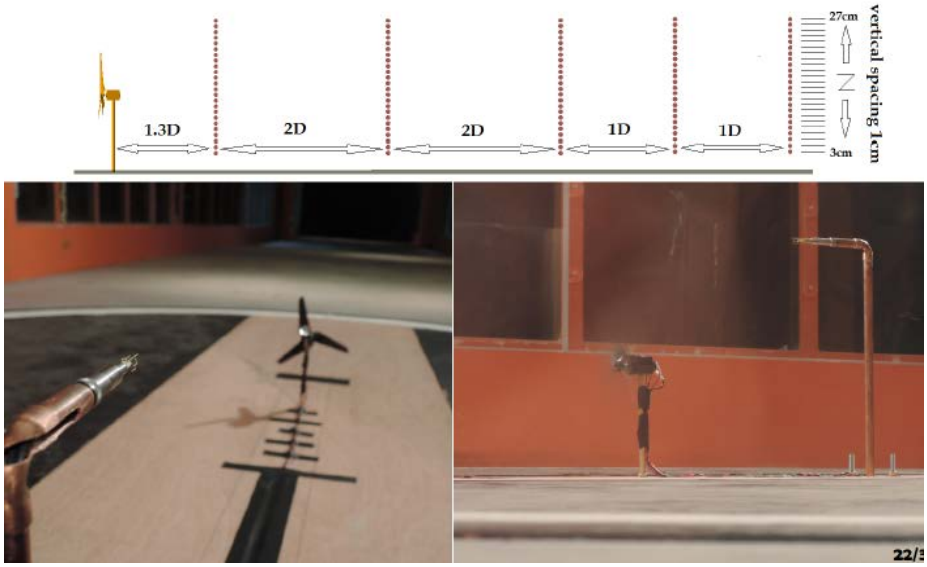

Figure 3: 3-component hot-wire anemometer installed in the VKI L1-B wind tunnel at offshore condition. Measurement locations are presented as dots. D is rotor diameter. Stereo-PIV equipment was installed outside the test section.

3 EXPERIMENTAL RESULTS FOR A SINGLE WIND TURBINE

Figure 3 shows the three-component hot-wire anemometer installed in the VKI L1-B wind tunnel, and the measurement locations. Inlet and wake flows are characterized in the symmetry plane for offshore (flat floor) and onshore (floor with 95mm high cups) conditions. Friction velocities are 0.56 m/s and 0.30m/s for offshore and onshore conditions, respectively. Roughness lenghs z_0 are 0.4 mm and 0.018 mm, whereas power law exponents read 0.3 and 0.16 for rough and smooth cases, respectively. The model wind turbine is always fully immersed in the boundary layer, being about 0.6m height (Conan 2012). Profiles of stream- and spanwise turbulence intensity and length scales are documented in Barlas et al (2015). Streamwise scales are about 2 times larger than the rotor diameter for the rough ABL and up to 6 times for the smooth ABL at tip height. Spanwise turbulent length scales are 0.4 and 0.6 times the rotor diameter, respectively. Turbulence intensities, defined with respect to hub height velocity, are about 5% and 15% for smooth and rough inflow cases, respectively.

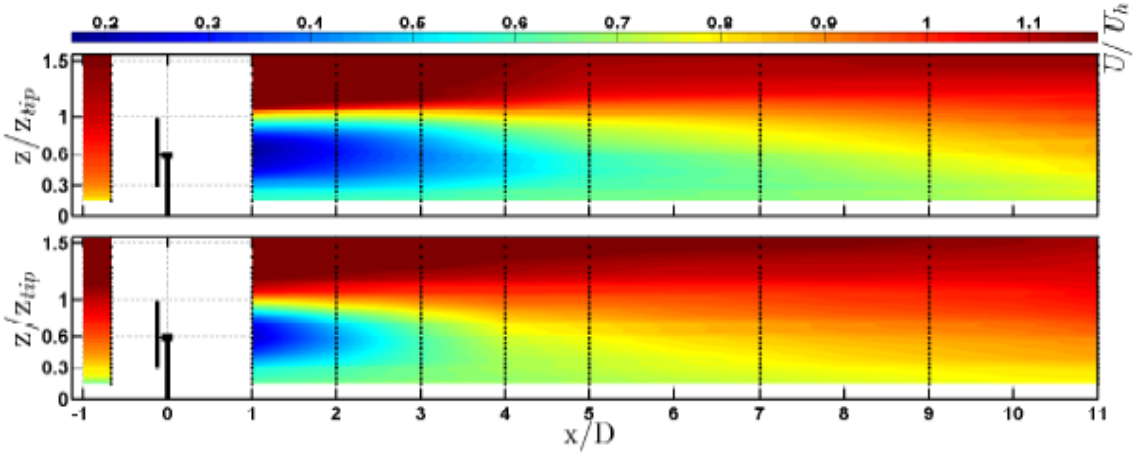

Figure 4: Normalized mean velocity maps (U/U_{hub}) as measured by hot wire anemometry for offshore (top) and onshore (bottom) conditions.

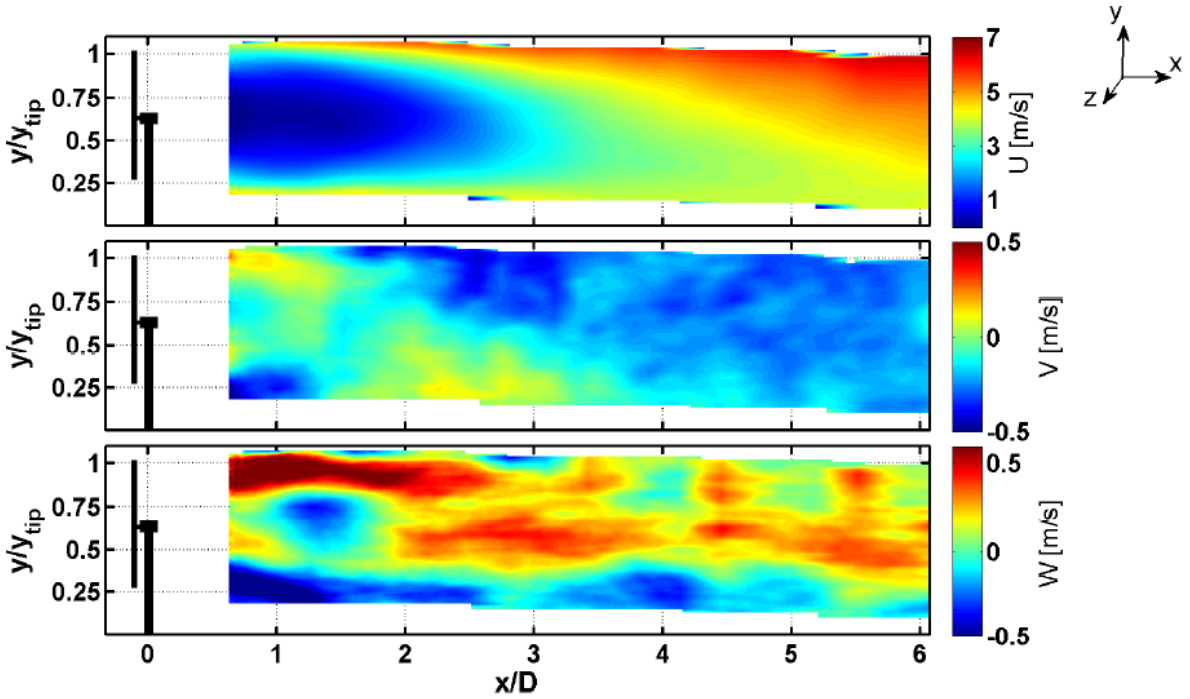

Figure 5: 3D Velocity maps as measured by stereo PIV for offshore conditions.

Figure 4 shows color plots of U/U_{hub} as measured by hot wire anemometry. Figure 5 shows stereo-PIV velocity fields for offshore case only, at 10Hz. Results are identical. Because 10Hz is insufficient to perform temporal analysis of the turbulent wind turbine wake, only 3D hot wire results were pursued.

The hot wire plots of Figure 4 clearly indicate an earlier wake recovery for the rough case, where the incoming turbulence is higher. The core of the wake is only effective up to 2.5 D for the rough case, while this value is around 4 D for the smooth one. However, the wake deficit does not lose its effect entirely as far as 11 D for neither of the cases. It is clear that the velocity distribution at the wake is not axisymmetric. This is expected as the incoming flow is not axisymmetric either. It is interesting to note that for the rough case, the velocity deficit recovers earlier to inflow velocity below the hub. This is contradictory with the recently published work on analytical wake modelling with Gaussian approach by Bastankhah and Porte-Agel (2014) which assumes an axysymmetric velocity deficit. Nevertheless, this is indeed the case for the smooth boundary layer.

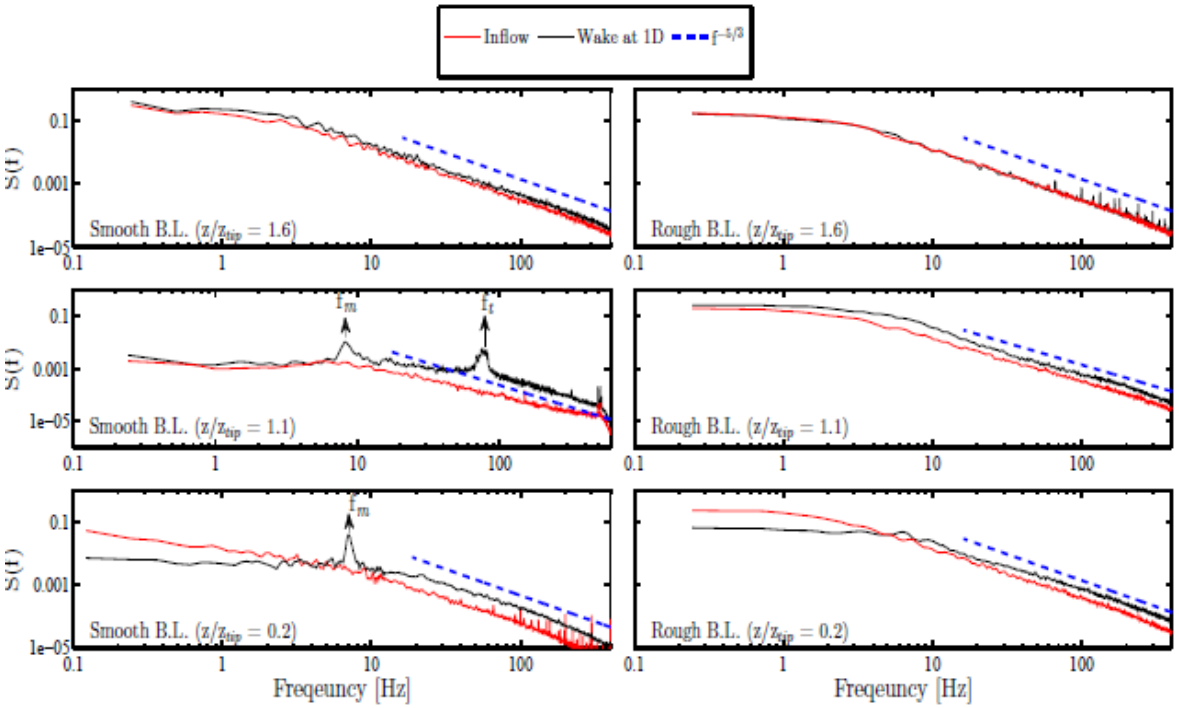

Figure 6: Energy spectrum of inflow (red) and wake at 1D distance (black) for offshore (left) and offshore ABL conditions. From top to bottom : above tip, tip and below hub.

Figure 6 shows the energy spectrum for the inflow and that in and above the turbine wake for both ABL conditions. It is observed that for both cases, the power of the very-large scale structures that exist in the incoming flow is decreased in the area below the nacelle, with a cut-off frequency of $f/f_t \sim 0{:}09$, with f_t being the turbine rotational frequency. This is in agreement with the value of 0.1 in Chamorro et al. (2012). Above this cut-off frequency the smaller scales gain in energy. Near the cut-off a low-frequency a peak appears, f_m, which represents meandering of the wake. Figure 7 shows the Strouhal number related to f_m as a function of the tip speed ratio. The Strouhal number varies around 0.25, which is a typical value for a bluff body (Sumer and Fredsoe 1997); Medici and Alfredsson (2008) found a Strouhal number of 0.13 for wake meandering behind their model wind turbines.

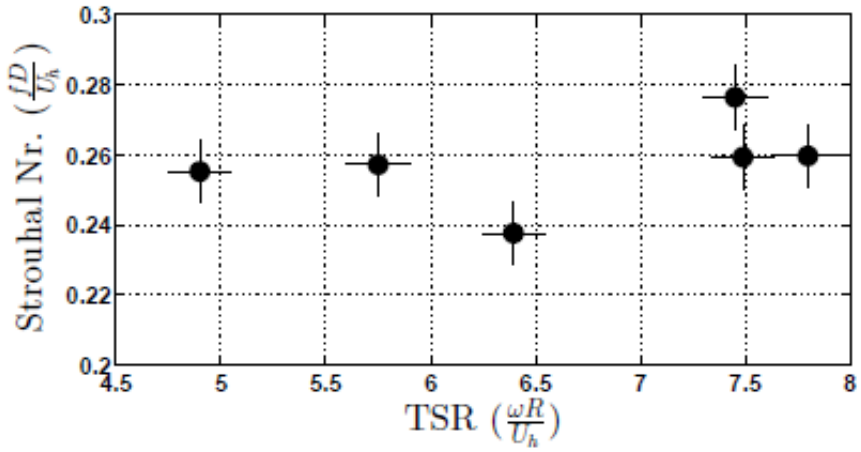

Figure 7: Strouhal number based on meandering frequency, rotor diameter and velocity at hub height as a function of the tip speed ratio.

Devinant et al. (2011) observed that meandering is very important when the incoming flow turbulence length scales are larger than the wake width. Larger scales where indeed visible for both ABL cases; however the incoming turbulence level was too high for the meandering to survive for the onshore "rough" case. This is clearly seen in Figure 8 and Figure 9, revealing spectrograms obtained from interpolating between the hot wire anemometry data following Chamorro et Porte-Agel, 2009, i.e. z/z_{tip} as a function of f/f_t. Figure 8 shows how the meandering frequency f_m acts as a filter and prevents the higher frequencies, such as the rotor frequency f_t, to disperse below f_m. Figure 9 shows the same for the rough ABL ("onshore"), however meandering is hardly visible within the incoming turbulence hence not dominant.

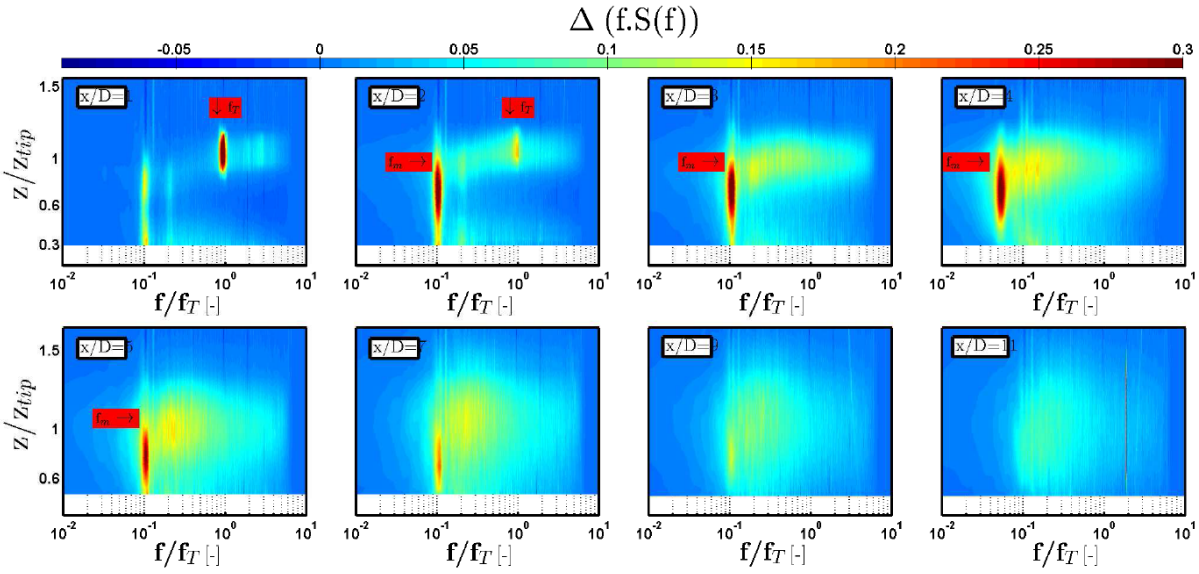

Figure 8: Spectral deviation from offshore inflow conditions at different locations in the wake after the first turbine row, assessed by hot wire anemometry, revealing a strong meandering frequency at about 1/10 of the rotor RPM, corresponding to a Strouhal number of 0.25, based on the rotor diameter.

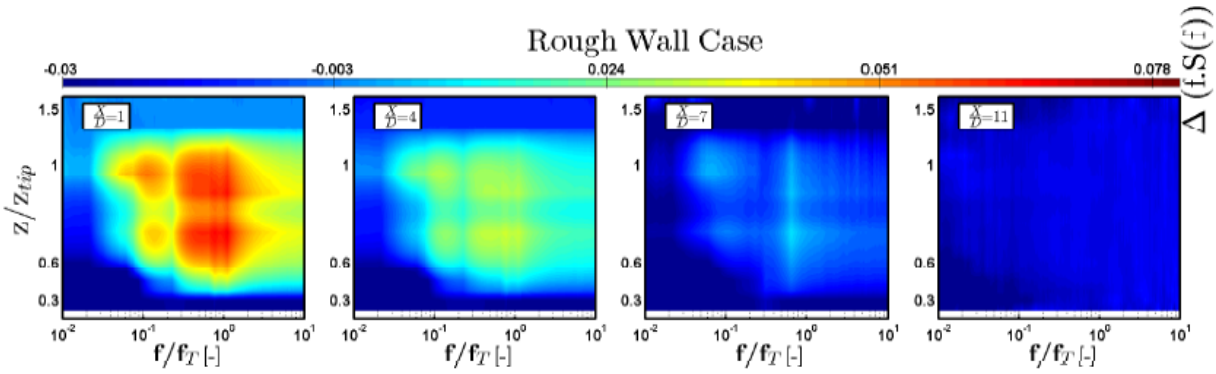

Figure 9: Spectral deviation from onshore inflow conditions at different locations in the wake after the first turbine row, assessed by hot wire anemometry, revealing a very weak meandering frequency at about 1/10 of the rotor RPM.

4 EXPERIMENTAL RESULTS FOR A 3X3 WIND FARM

A wind farm study with 9 turbines was carried out (Figure 10). Turbines were placed with 3 D and 5 D distances, in the span-wise and stream-wise directions. Hot wire measurements were taken at 4 D behind the mid turbine located at the last row. The results did not reveal any meandering frequency. Hence meandering did not persist further downstream in the model wind farm as studied in the VKI L1-B wind tunnel. Figure 11 shows horizontal mean and vertical mean velocities showing upwash after the first row and downwash after the second row, reflected in the larger power output for the third row with respect to the second one.

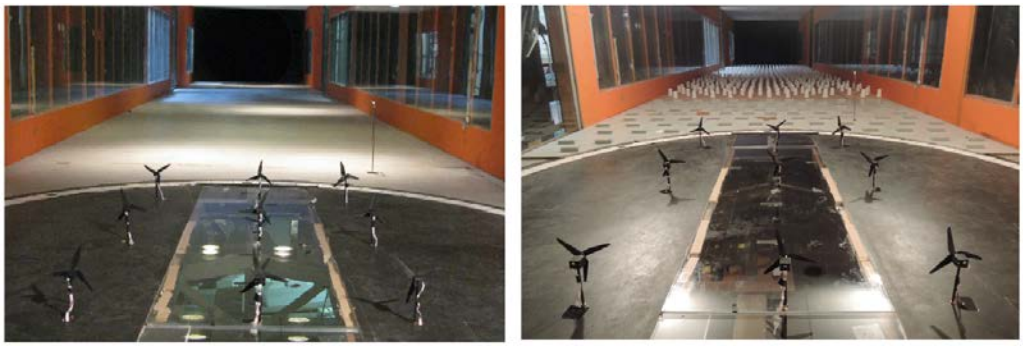

Figure 10: 3x3 wind turbine farm in offshore and onshore ABL conditions, installed in the VKI L1-B ABL wind tunnel.

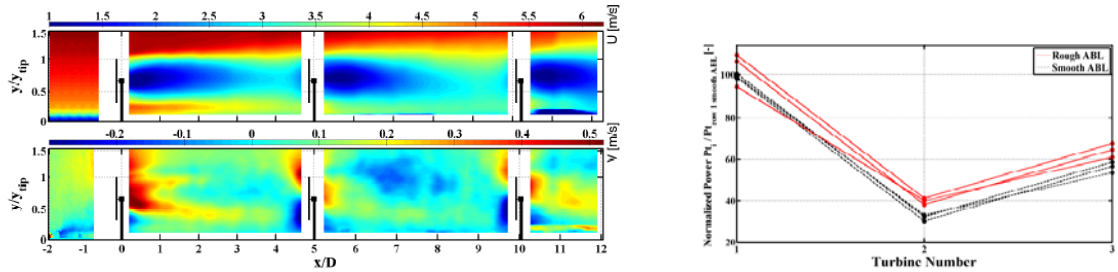

Figure 11: Mean velocity field, U (top) and V(bottom), in the 3x3 wind turbine farm in offshore ABL conditions, installed in the VKI ABL wind tunnel. Power output on the right.

5 CONCLUSIONS

Wind turbine models in the VKI ABL wind tunnel (L1-B) have been studied at offshore and onshore inflow conditions. For offshore conditions, i.e. low turbulence, the wind turbine wake turbulence is characterized by a meandering frequency, below which turbulence decreases and above which smaller scales have more power compared to upstream ABL inflow conditions. The Strouhal number related to wake meandering was 0.25. At onshore conditions and further downstream the wind farm, wake meandering turbulence is inferior to other turbulence structures.

6 REFERENCES

1. Bastankhah M, Porte-Agel F (2014). A new analytical model for wind-turbine wakes. Renewable Energy 70:116-123
2. B. Sanderse, S.P. van der Pijl, B. Koren (2011). Review of computational uid dynamics for wind turbine wake aerodynamics, Wind Energy - Special Issue: Wind Turbine Wakes, Volume 14, Issue 7, pages 799-819.
3. Chamorro L P, Porte-Agel F (2009). A Wind-Tunnel Investigation of Wind-Turbine Wakes: Boundary-Layer Turbulence Effects,. Boundary-Layer Meteorol 132:129-149.
4. Chamorro L P, Arndt R E A, Sotiropoulos F (2012). Reynolds number dependence of turbulence statistics in the wake of wind turbines. Wind Energy 15:733-742.
5. Church-field M J, Lee S, Michalakes J, Moriarty P J (2012). A numerical study of the effects of atmospheric and wake turbulence on wind turbine dynamics. J Turbulence 13:1-32.
6. Conan B (2012). Wind Resource Assessment in Complex Terrain by Wind Tunnel Modelling. Ph.D. thesis, VKI and Universite d'Orleans.
7. Crespo A, Hernandez J, Frandsen S (1999). Survey of modelling methods for wind turbine wakes and wind farms. Wind Energy 2:1-24.
8. Devinant P, Espana G, Loyer S., Aubrun S. (2011). Spatial Study of the Wake Meandering Using Modelled Wind Turbines In a Wind Tunnel. Wind Energy 14.7:923-937.
9. Gaumond M, Rethore P-E, Bechmann A, Ott S, Larsen G C, Pena Diaz A, Hansen K S (2012). Benchmarking of Wind Turbine Wake Models in Large Offshore Wind farms. Poster at The Science of Making Torque from Wind 2012, Oldenburg, Germany.
10. Larsen G C, Madsen H A, Thomsen K, Larsen T J (2008). Wake Meandering: A Pragmatic Approach. Wind Energy 11.4:377-395.
11. Medici D, Alfredsson P H (2008). Measurements behind model wind turbines; further evidence of wake meandering; Wind Energy 11:211-217, 2008.
12. Sumer B. M., Fredsoe J (1997) Hydrodynamics around cylindrical structures, World Scientific Publishing.
13. E. Barlas, S. Buckingham, J.P.A.J. van Beeck, 2015, Roughness Effects on Wind-Turbine Wake Dynamics in a Boundary-Layer Wind Tunnel, accepted for publication in Boundary Layer Meteorology